GeoStruct Innovations
https://www.acadlore.com/journals/GSI

Advanced Muck Pile Characterization for Optimized Blast Design and Excavator Loading Efficiency: A Synergistic Approach Using UAVs, PCA, and AI

Nidumukkala Sri Chandrahas[1*], Yewuhalashet Fissha[2,3], Nageswara Rao Cheepurupalli[3]

[1] Department of Mining Engineering, Malla Reddy Engineering College, 500014 Hyderbad, India
[2] Department of Geosciences, Geo-technology and Materials Engineering for Resources, Graduate School of International Resource Sciences, Akita University, 010-8502 Akita, Japan
[3] Mining Engineering Department, Aksum University, 7080 Aksum, Ethiopia

[*] Correspondence: Nidumukkala Sri Chandrahas (srichandru2009@gmail.com)

Received: 10-18-2024 **Revised:** 12-05-2024 **Accepted:** 12-20-2024

Citation: N. S. Chandrahas, Y. Fissha, and N. R. Cheepurupalli, "Advanced muck pile characterization for optimized blast design and excavator loading efficiency: A synergistic approach using UAVs, PCA, and AI," *GeoStruct. Innov.*, vol. 2, no. 4, pp. 190–210, 2024. https://doi.org/10.56578/gsi020402.

Abstract: Muck pile characteristics play a pivotal role in optimizing mining operations, particularly in understanding the post-blast behavior of throw, drop, and lateral spread, which directly impacts the selection and performance of loaders. The parameters of blast design are crucial in determining muck pile formation, influencing both loader efficiency and overall operational productivity. This study explores the effects of various blast design parameters on key muck pile attributes through a series of controlled blast experiments. Principal component analysis (PCA) was employed to identify the blast design factors most influential on muck pile characteristics, enabling the formulation of precise blast designs. The experiments were conducted across four phases at the OCI RGIII mines of Singareni Collieries Company Limited (SCCL), using advanced blast planning software to ensure accurate parameter implementation based on PCA results. Muck pile characteristics were assessed with the assistance of sophisticated artificial intelligence (AI) tools, providing valuable insights into blast optimization. The results revealed that blast designs incorporating a 1.35 spacing-to-burden (S/B) ratio, 0.9(B) stemming, 1-meter decking, and a V firing initiation pattern significantly enhanced muck pile performance. Specifically, these configurations reduced drop height by 3 meters, decreased throw distance by 5.9 meters, and increased lateral spread by 19.3 meters. These optimized muck pile attributes facilitated smoother loader operation, ultimately improving loading efficiency and the overall productivity of mining processes.

Keywords: Muck pile parameters; Artificial intelligence; Blast fragmentation; Unmanned aerial vehicle; Principal component analysis; Loader efficiency; Mining optimization

1 Introduction

The primary objective of rock fragmentation in mining is to reduce the size of the rock mass. The drilling and blasting processes create fragmented rock, which significantly affects the efficiency of downstream operations and the economic costs of mine production [1]. In addition to achieving optimal fragmentation size, factors such as throw, drop, and lateral spread of the muck pile are critical for determining the appropriate excavator for loading at the bench face.

The controlled detonation of explosives during blasting generates a shock wave that travels through the rock mass [2]. Following the blast, this shock wave fractures the material into smaller pieces, while the energy flow facilitates the spatial distribution of the shattered material [3]. The shape of the fragmented muck pile varies during blasting due to several factors, including burden, spacing, stemming length, decking length, and initiation pattern [4].

The dispersion process elucidates the drop of the explosion muck pile by detailing how fragments are disseminated and dispersed within the blast zone, encompassing their size, shape, and location. Additionally, geological discontinuities, such as the presence of joints at the bench, can alter fragmentation indices like drop, throw, and spread [5], as depicted in Figure 1.

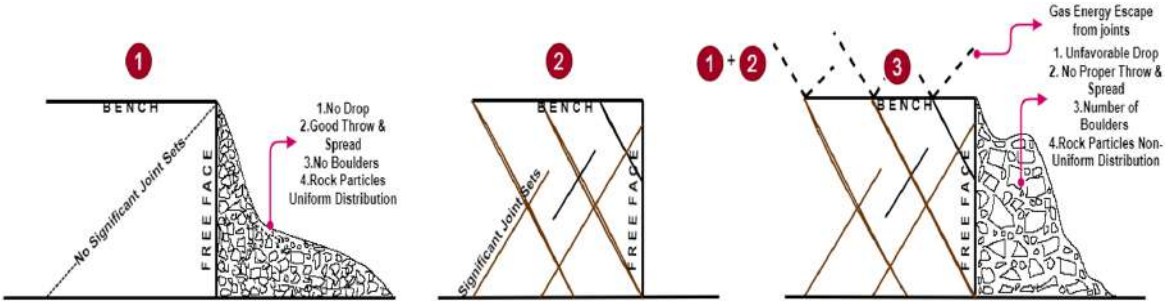

Figure 1. Impact of joints on rock fragmentation and muck pile characteristics

The degree and pattern of fragmentation can significantly influence subsequent processes such as transportation and crushing. Moreover, effective blast material distribution allows mine operators to improve output, reduce costs, and expand loading operations [6]. Modifying blast parameters according to rock conditions and geo-spatial contexts is essential for optimizing loading machine performance [7].

Researchers have examined fragmentation size distribution to better understand its effects on excavator loading performance and maintenance. Their findings indicate that fragmentation size should be optimized in relation to the excavator bucket size, enabling the excavator to load more material in less time. It has also been highlighted that optimal rock fragmentation and muck pile configurations are critical for maximizing an excavator's productive hours [1].

Consequently, it is vital to consider various factors when designing the blasting pattern, including burden, spacing, hole depth, stemming column, decking length, joint presence, and firing pattern [8–13]. Rock mass characteristics such as joint planes, spacing, and orientation significantly impact muck pile characteristics [14, 15]. The intricate relationships between rock factors and other controllable blast parameters that influence muck pile drop, throw, and spread have rendered the existing relationships and mathematical models inadequate for practical application [16].

2 Literature Review

The term "muck pile" refers to the fragmented material produced by the blasting process. The characteristics of muck piles are vital in mining blasting procedures, directly influencing the overall effectiveness and output of operations. Muck pile prediction is crucial for determining subsequent excavation and material handling steps [17]. Key attributes, such as particle size distribution, shape, and fragmentation, significantly impact loading and hauling efficiency, fragmentation analysis, and ore recovery efforts. Understanding and enhancing these characteristics is essential for optimizing blasting procedures and reducing costs related to material management. Irregularly shaped particles can increase friction and decrease flowability, leading to handling challenges and accelerated equipment wear [18].

Research on the drop, throw, and spread of muck piles during blasting has revealed significant variability due to factors like rock properties, blasting techniques, environmental conditions, and explosive characteristics. The drop refers to the vertical displacement of fragmented materials, influenced by explosive type, blast hole depth, and geological structure [19]. The throw indicates the horizontal distance traveled by the fragments, affected by blast design and explosive energy distribution. The spread represents the lateral extent of debris, influenced by terrain, blasting angle, and obstacles. Despite technological advancements, accurately predicting muck pile behavior remains challenging, highlighting the need for further research and empirical data to improve safety, efficiency, and sustainability in blasting practices [20].

2.1 Muck Pile Science Concerning Excavator Selection and Blast Design Parameters

Muck pile science is a multidisciplinary field that explores the characteristics of muck piles generated by mining explosive operations. Understanding these characteristics is crucial for selecting the right excavators for efficient material management [21]. The size, shape, and fragmentation of the muck pile directly influence the performance of various types of excavators. For example, a muck pile composed of large, irregularly shaped particles may require an excavator with a larger bucket capacity and greater breakout force to effectively handle and load the material [1]. Conversely, for a muck pile with a finer particle size distribution, an excavator with a smaller bucket may be more efficient for loading. By integrating muck pile science into excavator selection, mining companies can enhance operational efficiency and reduce costs associated with inefficient material handling.

Several studies have investigated the relationship between muck pile characteristics and excavator performance, as well as the influence of blast design parameters on muck pile properties. For instance, Chandrahas et al. [21] examined the effects of various blast design parameters on muck pile fragmentation in an open-pit mine. The findings

revealed that variations in explosive charge loading significantly affected the particle size distribution and morphology of the muck pile. Specifically, as the S/B ratio increased, the size of the blasted rock fragments decreased, resulting in an irregular muck pile shape concerning throw, drop, and spread [21]. This phenomenon may be attributed to the explosive's firing, which leads to a reduction in burden value and an increase in spacing [22]. Improved spacing combined with a lower burden resulted in thin ledges of rock mass, contributing to reduced fragmentation. The optimal S/B ratios for staggered and rectangular patterns were found to be 1.15 and 1.25, respectively, while typical ratios range from 1 to 2. Generally, the ideal S/B ratio for most blasts falls between 1.1 and 1.3, which produces good fragmentation and facilitates excavator selection [23].

A firing pattern provides the detonation waves with a designated path to reach the explosives within the holes. The periodic creation of a free face is a critical component of any blasting program. By enabling subsequent blast holes or rows to be positioned on a free face, the firing pattern establishes the movement and direction of the rock [24]. Additionally, research indicates that decking significantly influences how rocks move and evolve, especially in the presence of joints, ultimately affecting muck pile characteristics [25].

The formation of muck piles can vary considerably depending on the existence of fractures within the rock mass. Jointed benches are characterized by fractures and discontinuities, while non-jointed benches exhibit a more uniform rock structure. Recognizing the distinctions in muck pile formation between these two types of benches is vital for efficient blasting and material management [26]. Research has shown that muck piles from jointed benches tend to have larger particle sizes and irregular shapes compared to those from non-jointed benches [27]. Joints can provide preferential pathways for stress relief, resulting in the creation of larger fragments and irregularly shaped particles. The extent of jointing within a rock formation greatly influences the fragmentation shape and overall safety of the blasting operation [28]. Furthermore, the orientation of these joints can affect the propagation direction and intensity of fractures, thereby impacting the overall fragmentation characteristics of muck piles [29].

In another study, researchers explored the relationship between joint spacing and muck pile attributes in an open-pit mine. Their findings revealed that narrower joint spacing led to increased fracturing and fragmentation within muck piles. This highlights the necessity of incorporating joint characteristics into blasting designs to optimize fragmentation and improve material handling efficiency [30, 31]. Additionally, a separate investigation focused on how joint plane orientation influences muck pile fragmentation in coal mining. The results indicated that variations in joint plane orientation significantly affected the size distribution and shape of particles within muck piles, reinforcing the importance of including both joints and bedding planes in the optimization of explosive designs [32]. When the shock wave traveled at an angle to the joint plane, it resulted in suboptimal rock fragmentation. Conversely, when blasts were directed parallel to the planes of weakness, fragmentation improved. Many instances showed that aligning the free face parallel to the joint planes enhanced fragmentation and improved muck pile shape [33].

The effectiveness of subsequent loading, transportation, and crushing operations in open quarries is largely determined by the degree of muck pile fragmentation achieved through blasting. Thus, accurately predicting muck pile fragmentation prior to blasting is essential for operational success [34–38]. In these studies, various factors were analyzed, including S/B ratios, stemming lengths, decking lengths, firing patterns, explosive quantities, and joint conditions. Numerous researchers have identified a strong link between joint presence and the outcomes of successive blasting operations in rock [39].

3 Field Data Collection

Experiments were conducted at Opencast Mine I, Ramagundam, KLM Limestone Mine, and Kesoram Limestone Mine, all managed by SCCL, located in Telangana's South Godavari Basin, as illustrated in subgraph (a) of Figure 2 and subgraph (b) of Figure 2. These mines are positioned at latitudes 18°39'07" N and 18°41'05" N, and longitudes 79°32'37" E and 79°33'53" E. The mining area is enveloped by a notably thick layer of soil, alluvium, and sandy soil, along with various rocks belonging to the Barakar Formation of the Lower Gondwana Group.

The DJI MAVIC unmanned aerial vehicle (UAV) was employed to conduct imaging for the current assessment, capable of capturing both footage and photos in 4K resolution. Weighing 258 grams, the drone has a flight time of 25 minutes on a single battery charge. Signal tuning was performed to resolve issues, ensuring a successful drone launch, as illustrated in subgraph (a) of Figure 3, subgraph (b) of Figure 3 and subgraph (c) of Figure 3, which show a drone shot of the blast location in the limestone. The UAV was used to capture images of the benches from an orthogonal perspective before and after blast fragmentation. The primary objective of this drone survey was to obtain high-resolution photographs of the rock joint planes, joint spacing, and joint persistence along the vertical section of the bench. The UAV ascended to a height of 30.48 meters above the blast area, with a 75% overlap in its imaging.

To ensure flawless photographs, the camera angle was adjusted between 30 and 45 degrees to focus on the top edge and floor of the bench. Establishing a reliable 3D model for designing realistic blasts tailored to geological conditions relies heavily on selecting the appropriate acquisition axis. For this, the target bench was divided into three sections—top, bottom, and a combination of the crest and toe—allowing for optimal overlap of 70 to 80%.

Using Strayos software, the images captured by the UAV were processed to calculate the rock mass. Figure 4 depicts the entire process, from the initiation of UAV image acquisition to the identification of rock conditions through a developed 3D model.

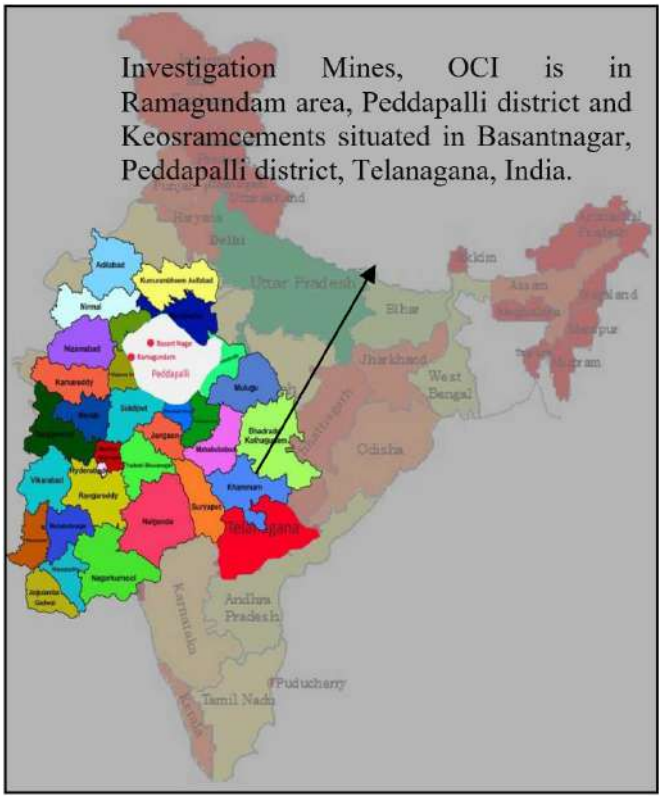

(a)

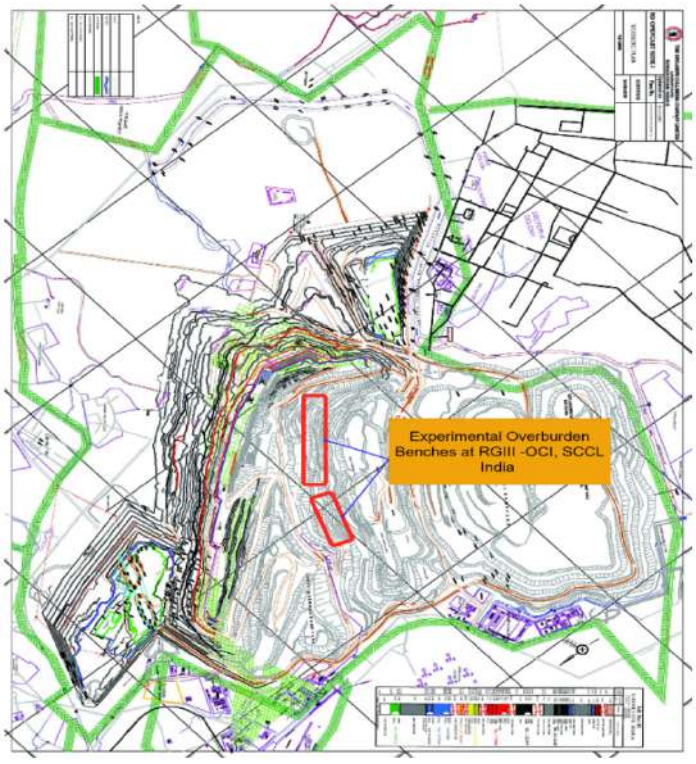

(b)

Figure 2. (a) Location of experiment sites on the India map, (b) Surface plan of OCI, SCCL

(a) (b) (c)

Figure 3. (a) Drone helipad with DJI MAVIC drone at OCI mine, Ramagundam Region, (b) DJI MAVIC drone flying at OCI, RGIII SCCL, to capture bench photographs, (c) GCP showing on bench top and floor at OCI SCCL, Ramagundam Region to create a 3D model for designing blasts

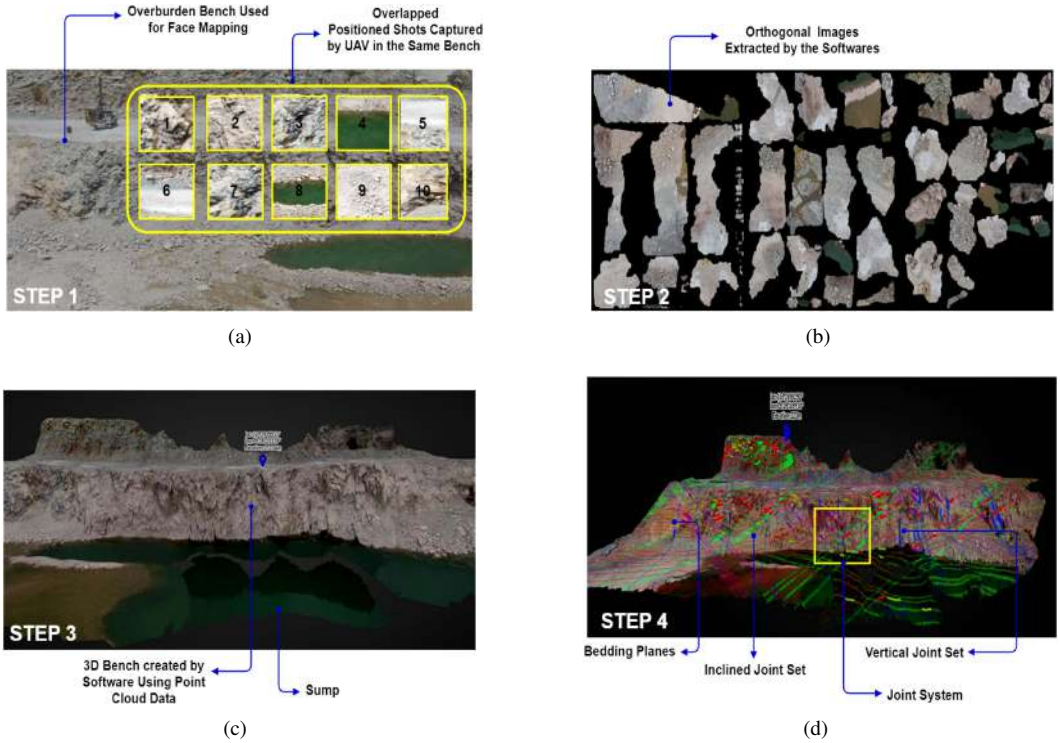

Figure 4. (a) Systematic representation of overlapping photos shot of UAV at OCI Mine, Ramagundam Region, (b) Ortho-sectional images extracted by software, (c) 3D model created by software using point cloud data, (d) Systematic bench 3D model representation with joint sets

Ground control points (GCPs) were established to define potential blasting site locations, with 4-5 GCPs marked on the surface using contrasting red digits to generate each 3D model, as shown in subgraph (c) of Figure 4. For broader coverage, GCP markers were placed in higher numbers at each site's outer corners. Due to the challenges of marking GCPs on fragmentation heaps, at least one GCP was designated for each elevation level, such as on the muck pile. The UAV operated and flew like a conventional aircraft.

The GCP markers must be collected, distortions avoided, and the camera kept in constant focus while recording flight footage. To create 3D models of blast benches, the data from the GCPs was imported into the software following targeted drone surveys.

The GCP data was prepared using the latitude and longitude of each GCP with the EPSG system. Utilizing EPSG 32644 and Strayos software, the GCP point data was saved in CSV format and transmitted along with the drone imagery. Once uploaded, the interface displays the geographical locations of the GCPs overlaid on satellite imagery, allowing users to verify and adjust their placements as shown in Figure 4. The ground sampling distance was set at 0.49 cm/pixel.

3.1 Joint Planes Analysis

To assess the joint intensity and patterns of the target bench, the rock mass AI Strayos software, which utilizes AI, was employed. The software's underlying algorithm is specifically designed to analyze data collections for features associated with rock joints. Images of rock joints are processed multiple times to identify distinct patterns within the gathered image data. Subgraph (d) of Figure 4 displays the three joint sets clustered during the plane analysis.

During the joint investigation, it was found that the rock formation at the Kesoram Limestone mines was significantly degraded and lacked uniformity. This limestone mine is one of the three trial sites with the highest number of joint planes. Users can activate the desired number of clusters based on their field experience, as well as the combined dip and strike of the planes for any clusters defined by the number of joints in the vertical section and the vertical spacing of spanning height joints (1, 2, 3, 4, 5, and 6). The joint planes and wire mesh view are illustrated in subgraph (a) of Figure 5 and subgraph (b) of Figure 5, with results presented in Table 1.

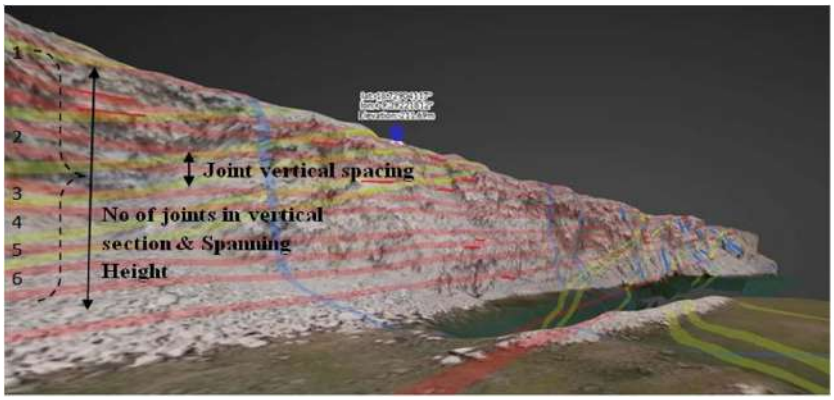

(a)

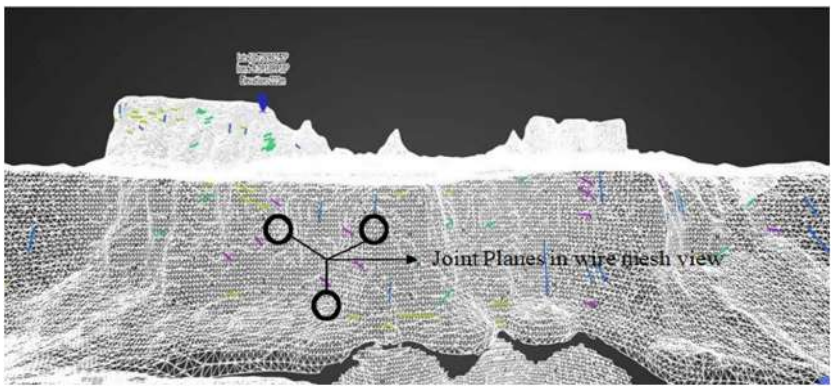

(b)

Figure 5. (a) Systematic view of joints in the bench, (b) Wire-meshed model of the bench at OCI, RGIII, SCCL

Table 1. Results of joint dip, strike directions and dip angle

Mine Name	No. of Benches	Bench Name	Set 1			Set 2			Set 3			Set 4			Set 5		
			D	S	DA	D	S	DA	D	S	DA	D	S	DA	D	S	DA
Opencast Mine - I	03	1A Seam	331	241	75	225	135	27	335	245	85	247	157	14	-	-	-
		2B Seam	220	130	26	298	208	30	305	215	30	221	131	30	-	-	-
		3A Seam	170	80	25	194	104	32	310	220	36	270	180	25	-	-	-
Opencast Mine - II	03	1A Top Seam	310	220	81	312	222	17	190	100	20	231	141	65	-	-	-
		II Seam	290	200	21	190	100	50	329	239	85	170	80	50	-	-	-
		3A Seam	200	120	24	300	210	73	250	160	41	184	94	71	-	-	-
Kesoram Limestone Mine	03	D Block	180	90	18	170	80	30	170	80	20	306	216	36	237	147	20
		G Block	319	229	78	320	230	70	310	220	69	231	141	72	212	122	38
		F Block	194	104	48	247	157	28	247	157	21	200	120	28	173	83	40

Note: D indicates the dip direction; S indicates the strike direction, and DA indicates the dip angle.

3.2 PCA

In the current investigation, PCA was conducted using XLSTAT to understand how independent and dependent variables influence trends for the final blast design to be employed in experimental blasts. The input data for blast design parameters included hole diameter, burden, spacing, front row burden, decking, stemming, firing pattern, total average explosive quantity, and total explosive quantity. Additionally, geotechnical parameters, such as joint spacing, joint gap, joint angle, joint number, and joint spanning height, were selected for the PCA.

The technical information regarding joints used in the PCA was obtained from AI-based software, which collected data during the initial site visit, as detailed in Table 1.

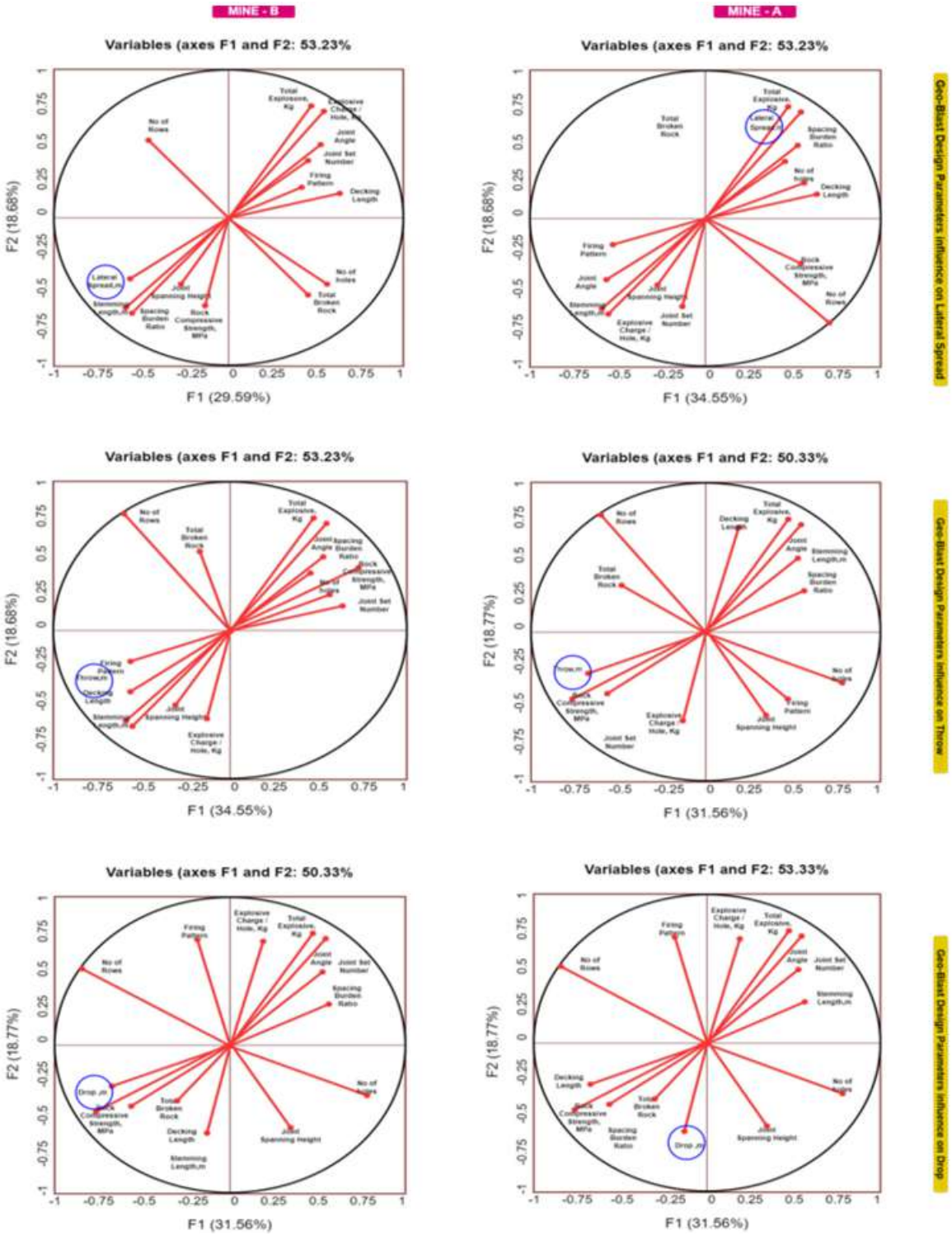

Figure 6. Throw, drop and lateral spread correlation circle diagram of mines A & B

The interpretation of PCA begins with the correlation circle produced by XLSTAT, which provides values guiding further analysis. The correlation circle is essential for examining the relationships between independent and dependent variables. The interpretation is divided into three segments: positively correlated, negatively correlated, and orthogonally correlated. Variables located closely in the same quadrant are considered positively correlated, while those positioned in opposite quadrants are negatively correlated, and those adjacent to each other are orthogonally related. A positive correlation indicates a proportional relationship, a negative correlation suggests an inversely proportional relationship, and orthogonal variables imply no relationship among them. XLSTAT was used to analyze the relationship between mean fragmentation size and peak particle velocity (the dependent variable) with various independent variables, including burden, spacing, front row burden, stemming, decking, hole depth, and explosive quantity.

The parameters analyzed through PCA aimed to determine the degree of correlation and grouping among the various variables and observations. Blasting operations are influenced by numerous interacting factors that collectively produce blast effects. Considering only one or two factors would yield incomplete findings. Therefore, PCA serves as a valuable tool for enhancing the understanding of blasting fragmentation and muck pile characteristics by linking multiple factors together. The PCA of the relationships among parameters is illustrated in Figure 6.

It was found that, with the exception of the number of rows, holes, rock compressive strength, and total rock broken, most baseline input parameters displayed either a positive or negative correlation with muck pile parameters.

3.3 Blast Design, Prediction, and Field Experimentation

In relation to the study's objectives, each of the 32 blasts was designed based on the presence of joint planes, dip-strike directions, and the corresponding sectional rock compressive strengths derived from PCA-filtered data. The charge and decking lengths were adjusted in Strayos software to predict rock fragmentation and muck pile characteristics, as illustrated in Figure 7. The software operates based on the KUZ-RAM and SWEBREC models to forecast outcomes.

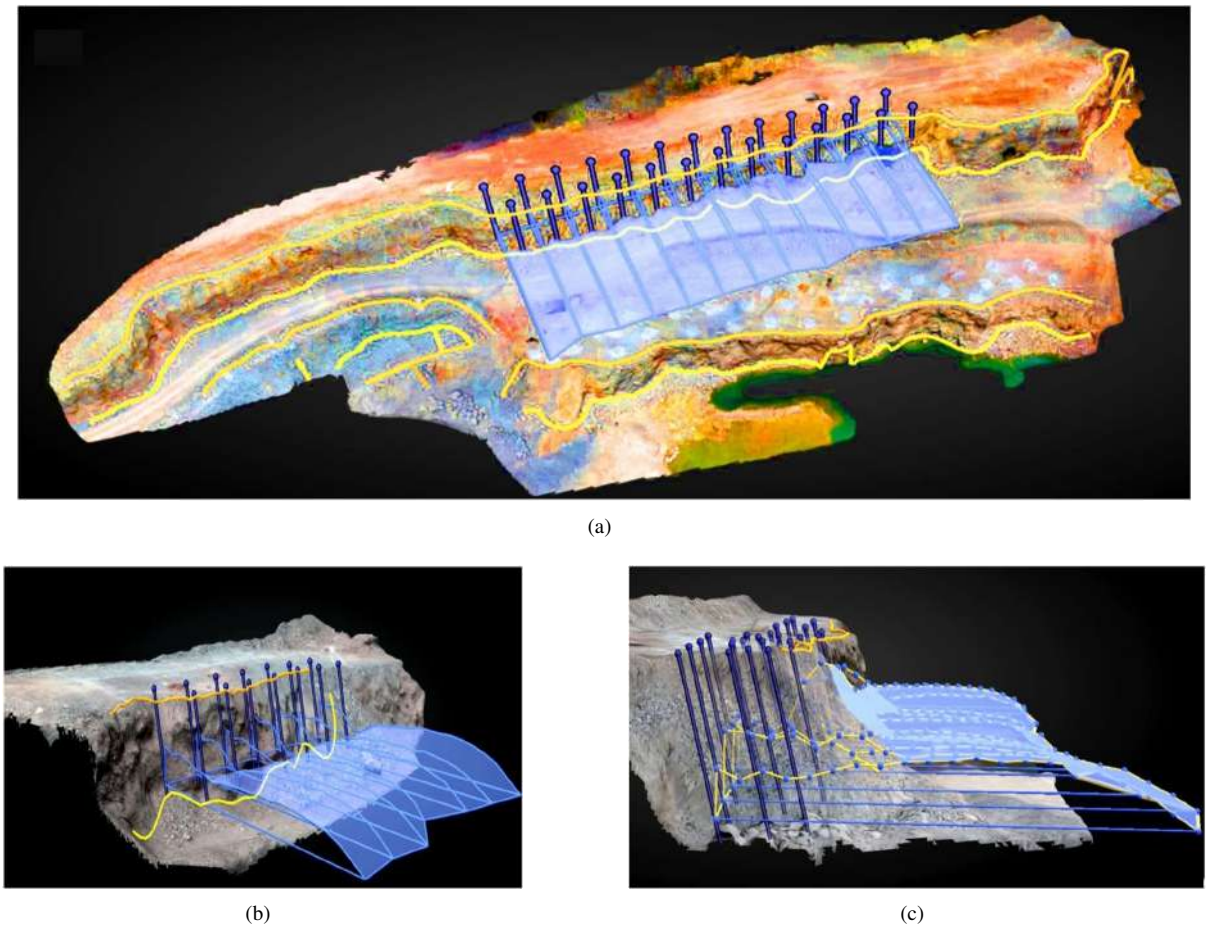

(a)

(b)

(c)

Figure 7. (a) Isometric view of the 3D model generated by software, (b) Isometric view of muck pile prediction for respective blast design, (c) Cast analysis of muck pile prediction

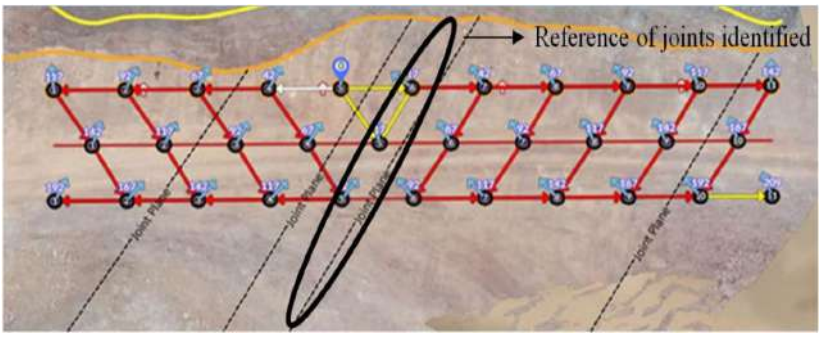

(a)

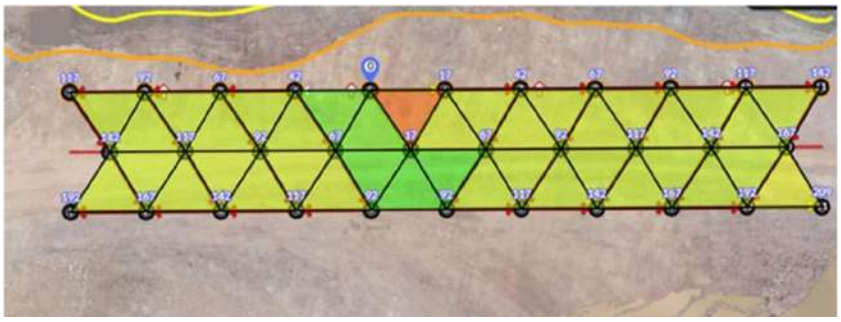

(b)

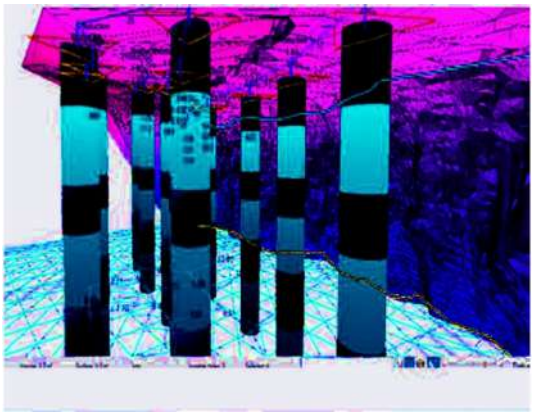

(c)

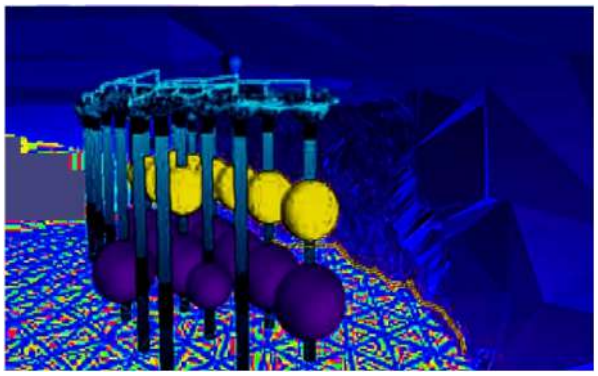

(d)

Figure 8. (a) V firing initiation flow and throw prediction of KLM site blasts, Telangana, (b) Design of V firing pattern with joint references identified of KLM, Telanagana, (c) Blast hole charging interface, (d) Multi-decking and initiation design and prediction in AI blasting software

The phases are designated I, II, III, and IV, as seen in the following explanation:

Phase I: All blast design parameters are maintained the same, but the firing pattern is altered with respect to joint angle.

Phase II: All blast design parameters are maintained the same, but the S/B ratio is altered with respect to joint angle.

Phase III: All blast design parameters are maintained the same, but the explosive quantity and decking length are altered with respect to the rock compressive strength.

Phase V: All blast design parameters are maintained the same, but the firing pattern and S/B ratio together are altered concerning the joint angle.

In the blast design process for all investigated mines, three distinct initiation patterns—line, diagonal, and V patterns—were identified as the most common choices. Accordingly, all models were developed using a scaled reference of joint planes aligned with the dip and strike directions identified in the geological analysis, as demonstrated in rock mass AI Strayos software, with relevant data shown in Table 1 and subgraph (d) of Figure 4.

In addition to joint direction and presence, the number of joints and joint spanning height are crucial factors to consider during burden spacing. This approach ensures that drill holes in joint planes do not overlap, which could lead to drill jams and adversely impact the economics of the blast. Throughout the investigation, all parameters were kept constant to assess the influence of various combinations on fragmentation and muck pile characteristics. Consequently, the initiation accessories and sequence timings used in all blasts were standardized as much as possible. Predictions for muck pile drop, throw, and spread are illustrated in Figure 7 along with excavator selection, while blast hole charging and initiation are depicted in subgraph (c) of Figure 8 and subgraph (d) of Figure 8.

A total of 164 blasts were conducted at two testing locations over 45 days, with decking lengths adjusted according to joint spanning heights. In coal mines, blasting is typically executed using down-hole delays of 425 and 450 milliseconds, hole-to-hole delays of 17 milliseconds, and row-to-row delays of 25 and 42 milliseconds, with V firing patterns employed as necessary based on rock conditions, as shown in subgraph (a) of Figure 8 and subgraph (b) of Figure 8. Site mixed emulsion (SME) explosives were used in combination with a booster-NONEL setup, while limestone benches utilized ANFO. Typically, two boosters were deployed for every meter of hole depth, and the average explosive usage rate ranged from 45 to 55 kg. The muckpile characteristics predictions were presented in Figure 9.

In the case study of limestone benches, the typical explosive charge per hole for ANFO-charged holes was 18 kg, accompanied by five to six boosters. All experiments conducted in this study involved blasts at OCI, utilizing SME explosives. The initial density was maintained between 1.25 g/cc and 1.29 g/cc, while the final density reached between 1.05 g/cc and 1.1 g/cc after a gassing period of 20 to 25 minutes.

Pentolite boosters were incorporated into each blast hole at a rate of 0.2% of the total SME explosives to enhance energy discharge. To ensure a high rate of energy release, the viscosity of the SME explosives was kept within the range of 40,000 to 80,000 cps. Experimental photographs and detailed blast information are presented in Figure 10 and Table 2.

Table 2. Blast design parameters and results

S.No	Pattern	Phases	Blast Design Parameters							
			Blast No.	No. Rows	No. Holes	Hole Diameter, mm	Average Hole Depth, m	S/B Ratio (Se/Be), m	Front Row Burden, m	Stemming Length, m
1	FP altered All same	Phase - I	A1	3	30	150	12	1.3	2.5	4.5
2			A2	3	30	150	12	1.3	2.5	4.5
3			A3	3	23	150	12	1.3	2.5	4.5
4			A4	3	30	150	12	1.3	2.5	4.5
5			A5	3	28	150	12	1.3	2.5	4.5
6			A6	3	27	150	12	1.3	2.5	4.5
7			A7	3	30	150	12	1.3	2.5	4.5
8			A8	3	30	150	12	1.3	2.5	4.5
9	Se/Be ratio altered All same	Phase - II	B1	3	28	150	12	1.2	2.5	4.5
10			B2	3	30	150	12	1.2	2.5	4.5
11			B3	3	28	150	12	1.2	2.5	4.5
12			B4	3	30	150	12	1.3	2.5	4.5
13			B5	3	28	150	12	1.3	2.5	4.5
14			B6	3	27	150	12	1.3	2.5	4.5
15			B7	3	27	150	12	1.35	2.5	4.5
16			B8	3	30	150	12	1.35	2.5	4.5

S.No	Pattern	Phases	Blast Design Parameters							
			Blast No.	No. Rows	No. Holes	Hole Diameter, mm	Average Hole Depth, m	S/B Ratio (Se/Be), m	Front Row Burden, m	Stemming Length, m
17			C1	3	27	150	12	1.3	2.5	4.5
18			C2	3	30	150	12	1.3	2.5	4.5
19	EQ &		C3	3	28	150	12	1.3	2.5	4.5
20	SL		C4	3	27	150	12	1.3	2.5	5.5
21	altered	Phase - III	C5	3	27	150	12	1.3	2.5	5.5
22	All		C6	3	30	150	12	1.3	2.5	5.5
23	same		C7	3	30	150	12	1.3	2.5	6
24			C8	3	27	150	12	1.3	2.5	6
25			C9	3	27	150	12	1.3	2.5	6
26			D1	3	27	150	12	1.3	2.5	4.5
27			D2	3	30	150	12	1.3	2.5	4.5
28	EQ		D3	3	26	150	12	1.3	2.5	4.5
29	& DL	Phase - IV	D4	3	28	150	12	1.3	2.5	4.5
30	altered		D5	3	27	150	12	1.3	2.5	4.5
31	All		D6	3	27	150	12	1.3	2.5	4.5
32	same		D7	3	27	150	12	1.3	2.5	4.5
33			D8	3	27	150	12	1.3	2.5	4.5
34			E1	3	27	150	12	1.25	2.5	4.5
35	FP &		E2	3	27	150	12	1.25	2.5	4.5
36	Se/Be		E3	3	30	150	12	1.25	2.5	4.5
37	ratio		E4	3	27	150	12	1.35	2.5	4.5
38	together	Phase - V	E5	3	27	150	12	1.35	2.5	4.5
39	altered		E6	3	27	150	12	1.35	2.5	4.5
40	All		E7	3	27	150	12	1.4	2.5	4.5
41	same		E8	3	30	150	12	1.4	2.5	4.5
42	DL,		G1	3	26	150	12	1.3	2.5	4.5
43	EQ		G2	3	31	150	12	1.3	2.5	4.5
44	& FP		G3	3	25	150	12	1.3	2.5	4.5
45	altered		G4	3	28	150	12	1.3	2.5	4.5
46	All	Phase - VI	G5	3	27	150	12	1.3	2.5	4.5
47	same		G6	3	27	150	12	1.3	2.5	4.5
48			G7	3	27	150	12	1.3	2.5	4.5
					Mine B					
49			A17	3	30	150	12	1.3	2.5	4.5
50			A18	3	28	150	12	1.3	2.5	4.5
51	FP		A19	3	27	150	12	1.3	2.5	4.5
52	altered		A20	3	30	150	12	1.3	2.5	4.5
53	All	Phase - I	A21	3	28	150	12	1.3	2.5	4.5
54	same		A22	3	27	150	12	1.3	2.5	4.5
55			A23	3	27	150	12	1.3	2.5	4.5
56			A24	3	23	150	12	1.3	2.5	4.5
57			B17	3	23	150	12	1.2	2.5	4.5
58	Se/Be		B18	3	28	150	12	1.2	2.5	4.5
59	Ratio		B19	3	27	150	12	1.2	2.5	4.5
60	altered		B20	3	27	150	12	1.3	2.5	4.5
61	All	Phase - II	B21	3	30	150	12	1.3	2.5	4.5
62	same		B22	3	27	150	12	1.3	2.5	4.5
63			B23	3	27	150	12	1.35	2.5	4.5
64			B24	3	30	150	12	1.35	2.5	4.5
65			C19	3	28	150	12	1.3	2.5	4.5
66			C20	3	31	150	12	1.3	2.5	4.5
67	EQ		C21	3	30	150	12	1.3	2.5	4.5
68	& SL		C22	3	27	150	12	1.3	2.5	5.5
69	altered	Phase - III	C23	3	28	150	12	1.3	2.5	5.5
70	All		C24	3	31	150	12	1.3	2.5	5.5
71	same		C25	3	30	150	12	1.3	2.5	6
72			C26	3	27	150	12	1.3	2.5	6
73			C27	3	27	150	12	1.3	2.5	6

S.No	Pattern	Phases	Blast Design Parameters							
			Blast No.	No. Rows	No. Holes	Hole Diameter, mm	Average Hole Depth, m	S/B Ratio (Se/Be), m	Front Row Burden, m	Stemming Length, m
74			D17	3	27	150	12	1.3	2.5	4.5
75			D18	3	30	150	12	1.3	2.5	4.5
76	EQ &		D19	3	26	150	12	1.3	2.5	4.5
77	DL		D20	3	28	150	12	1.3	2.5	4.5
78	altered	Phase - IV	D21	3	27	150	12	1.3	2.5	4.5
79	All		D22	3	26	150	12	1.3	2.5	4.5
80	same		D23	3	30	150	12	1.3	2.5	4.5
81			D24	3	27	150	12	1.3	2.5	4.5
82			E17	3	27	150	12	1.25	2.5	4.5
83	FP &		E18	3	27	150	12	1.25	2.5	4.5
84	Se/Be		E19	3	30	150	12	1.25	2.5	4.5
85	ratio	Phase - V	E20	3	27	150	12	1.35	2.5	4.5
86	together		E21	3	30	150	12	1.35	2.5	4.5
87	altered		E22	3	29	150	12	1.35	2.5	4.5
88	All		E23	3	27	150	12	1.4	2.5	4.5
90	same		E24	3	28	150	12	1.4	2.5	4.5
91			G15	3	26	150	12	1.3	2.5	4.5
92	DL,		G16	3	31	150	12	1.3	2.5	4.5
93	EQ &		G17	3	30	150	12	1.3	2.5	4.5
94	FP		G18	3	27	150	12	1.3	2.5	4.5
95	altered	Phase - VI	G19	3	30	150	12	1.3	2.5	4.5
96	All		G20	3	27	150	12	1.3	2.5	4.5
97	same		G21	3	26	150	12	1.3	2.5	4.5

Table 3. Blast design parameters and results (Table 2 continued)

Blast Design Parameters			Joint Features			Muck Pile Characteristics		
Average Explosive per Hole, kg	Total Explosive, kg	Firing Pattern	Joint Spanning Height, m	Joint Angle	Joint Set Number	Drop, m	Throw, m	Spread
390	11,700	1	1.5	70	1	7.7	2.3	12.3
	11,700	1	3.5	66	1	9	6.1	23.3
	8,655	1	3	53	1	11	5.3	15.3
	11,700	2	4	68	1	9	3.3	14.6
	10,460	2	4	32	1	12	4.1	13.4
	9,940	1	4.2	58	2	9	2.5	12.8
	11,700	3	3	90	2	5	1.6	13.8
	11,700	3	3.6	32	2	3	5.9	19.3
390	105460	1	1	53	2	6	2.5	14.6
	11,600	1	1.3	54	2	8	4.3	20.5
	10,450	1	3	62	3	4	3.1	12.8
	11,600	1	2.9	34	3	11	5.8	13.9
	10,700	1	1.4	32	2	12	2.1	14.2
	9,700	1	2.7	45	1	7	4.2	20.1
	9,950	1	2.5	634	1	5	5.8	13.1
	11,500	1	3.4	55	2	8	2.3	21.3
390	9,890	3	5.8	46	2	9	4.3	14.1
	11,800	3	4.6	75	2	7.5	5.7	22.1
	10,920	3	5.32	85	2	8	3.3	15.3
325	7,020	3	2	90	2	5.8	2.4	23.5
	8,775	3	3.1	45	2	8	4.4	16.5
	9,750	3	2	47	1	5.7	5.6	17.9
292	11,780	3	4.72	84	2	9	4.10	24.5
	7,884	3	3.8	52	2	7	5.11	26.5
	7,860	3	2	53	2	8.3	2.5	22.1

Blast Design Parameters			Joint Features			Muck Pile Characteristics		
Average Explosive per Hole, kg	Total Explosive, kg	Firing Pattern	Joint Spanning Height, m	Joint Angle	Joint Set Number	Drop, m	Throw, m	Spread
335	9,045	2	2.5	65	2	7	4.5	15.3
	9,756	2	2.9	67	2	6.9	5.5	13.3
	8,455	2	5.7	72	1	9.3	3.4	12.6
257	7,280	2	4.8	48	1	11	2.6	16.5
	7,020	2	2	73	1	12.5	3.7	17.6
	5.670	2	3.7	55	2	7.9	5.5	21.1
210	5,660	2	2	59	3	9.2	2.7	15.4
	5,655	2	2.1	82	1	8	4.6	16.5
465	12,555	1	2	53	2	6	5.4	22.3
	13, 950	1	2	65	1	5	2.6	20.9
	12,560	1	2.4	62	1	5.9	3.8	21.9
	12,470	2	2	57	3	9.4	5.6	15.9
	12,400	2	2.6	58	3	8	4.7	14.7
	13,621	3	1.4	90	3	7.7	2.8	12.5
	12,500	3	5.21	32	3	8	3.8	21.8
	13.800	3	6	19	3	5.9	4.8	26.6
325	8,800	3	4.65	43	2	7	5.4	23.3
	9,830	3	2	26	3	6.9	2.9	21.3
	8,521	2	4	42	3	8	3.8	22.3
265	7,255	2	2.3	47	3	8	4.5	18.6
	7,200	3	2	75	3	8	5.3	17.8
220	5,940	1	2	71	3	6	2.10	12.4
	5,900	1	2.7	47	3	4	4.10	13.6
				Mine B				
140	4,200	2	2.04	55	2	8.9	2.1	14.8
	3,920	2	5	41	2	6.8	4.5	15.8
	3,780	2	3	37	2	5	3.8	13.6
	4,200	1	3	84	3	8	5.4	12.8
	3,820	1	5.4	37	2	2.8	5.10	21.6
	3, 800	3	2.6	58	2	8	3.5	25.8
	3, 790	3	3.7	69	2	7.6	2.5	12.1
	3,220	3	4	55	3	8	4.6	15.5
145	3,335	2	4.3	34	3	8	2.10	16.4
	4,060	2	4	63	3	8	3.2	21.6
	3,915	2	1.2	57	2	8.5	4.6	25.6
	3,900	2	5	65	3	5	5.10	21.8
	4,350	2	1.32	45	3	5	2.8	12.6
	3,920	2	5.34	34	3	5	3.6	17.6
	3,932	2	3	65	2	5	2.4	13.4
	3,913	2	3.12	77	3	6	4.2	19.5
140	3,920	1	2	65	2	3	5.5	19.3
	4,340	1	2.4	35	3	5	2.6	21.1
	4,200	1	2.1	44	2	5	3.1	20.5
120	3,250	1	3	47	2	5	2.8	13.6
	3.360	1	3	85	2	5	4.7	20.6
	3,720	1	2.5	66	2	9	5.8	16.7
110	3,300	1	3	37	3	9	2.4	14.8
	2,970	1	1.1	51	2	5.6	3.8	15.9
	2,980	1	4.3	57	2	6	4.9	12.9
100	2,700	1	4.1	85	2	6	5.6	21.9
	3,000	1	4	44	2	6	2.1	20.3
	2,600	1	1.5	35	2	6.8	3.8	15.7
80	2,240	1	3.5	64	1	9.4	5.3	13.4
	2,160	1	3	35	1	6	3.3	12.4
	2,080	1	4	75	1	6	4.8	23.5
60	1,800	1	2.4	74	1	6	2.1	25.9
	1,620	1	2	34	1	6	5.9	13.6
	3,780	3	2.6	66	1	6	2.8	14.9

Blast Design Parameters			Joint Features			Muck Pile Characteristics		
Average Explosive per Hole, kg	Total Explosive, kg	Firing Pattern	Joint Spanning Height, m	Joint Angle	Joint Set Number	Drop, m	Throw, m	Spread
140	3,790	3	1.4	25	1	9	2.10	16.3
	4,200	3	5.21	37	1	9	4.8	17.8
	3,810	1	6	58	1	5.6	2.6	19.5
	4,210	1	5.7	64	2	6.3	3.5	25.4
	4,060	2	5.32	47	2	8	5.5	12.7
	3,800	2	1	85	2	6	4.6	13.4
	3,920	2	3.2	44	2	3	5.4	16.5
110	2,860	1	2	35	2	7	3.7	18.3
	3,410	1	2	78	2	9	5.3	17.5
	3,300	2	2.7	67	2	3	4.3	22.5
100	2,700	2	3.2	90	2	6	2.5	25.3
	3,000	2	3.9	47	1	8.7	4.7	22
	2,430	3	2.7	88	2	9	3.8	15.6
	2,340	3	3.2	85	2	9	2.9	18

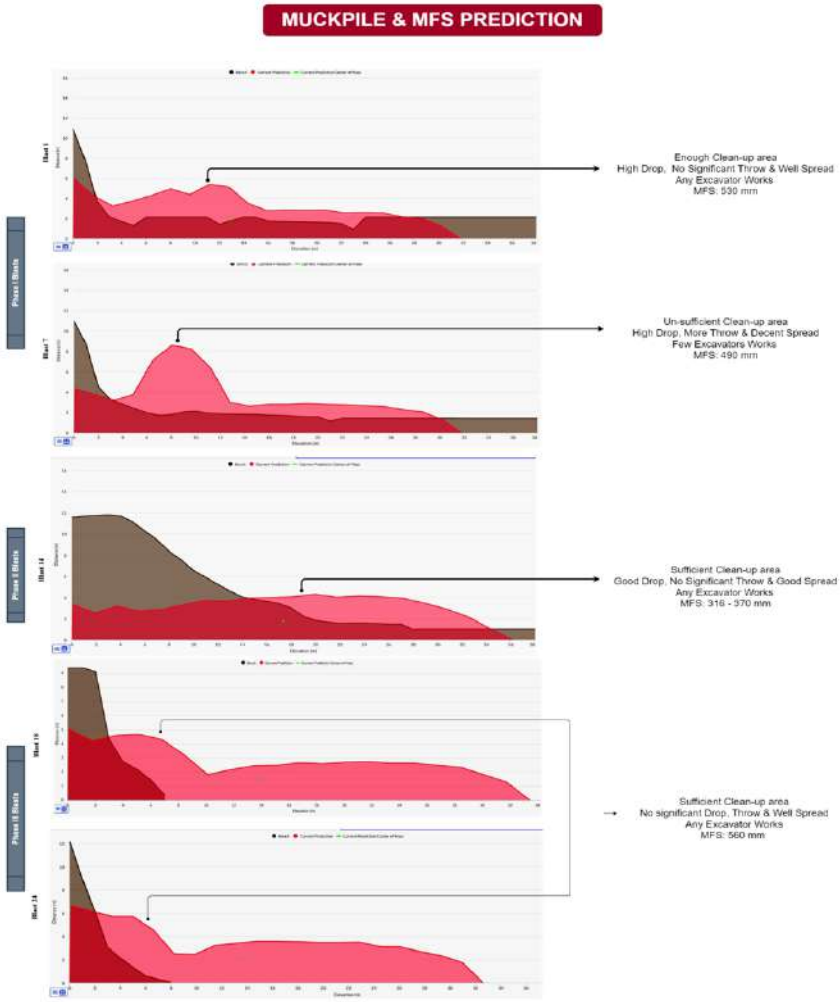

Figure 9. Muck pile characteristics (drop, throw and lateral spread prediction in software) for a few blasts to understand the trend and impact on the loader

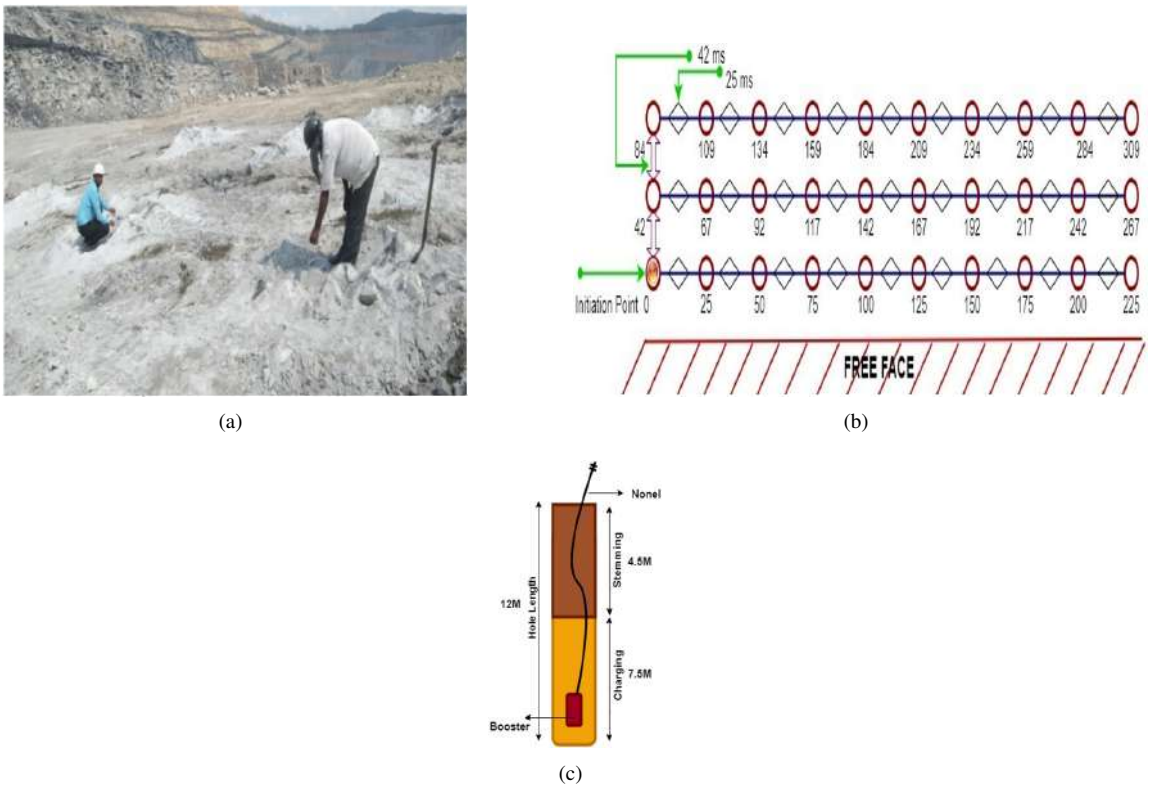

(a) (b) (c)

Figure 10. (a) Burden spacing measurement at OCI, RGIII, SCCL, (b) Rectangular drilling with diagonal firing pattern at the mine, (c) Blast hole section at the mine

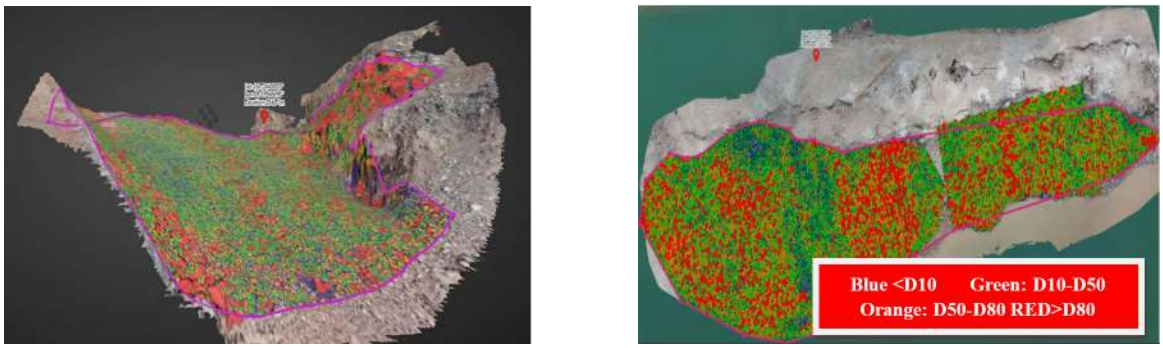

(a) (b)

Figure 11. (a) Rock fragmentation analysis of the 3D model in Strayos software, (b) Rock fragmentation analysis of the 2D model in Strayos software

3.4 Fragmentation and Muck Pile Measurement

In the AI-based software, the concepts of KUZ-RAM and SWEBREC were employed to calculate values such as D10, D20, D80, and D90. Each subsequent 3D model of rock fragmentation was generated using approximately 10 to 15 high-quality source images, as shown in Figure 11. After the detonation at midday, the drone was flown over the muck pile at a height of 90 feet, with a camera angle of 90 degrees, perpendicular to the ground, ensuring 80 percent overlap in the images. This approach was taken to avoid overlapping shadows and prevent dust from accumulating on the rocks. The fragmentation distribution graph and particle size dimensions are presented in Figure 12.

In the current study, a novel approach to muck pile measurement was implemented to enhance accuracy and reduce processing time. Features of the muck pile, including drop, throw, and lateral spread, were quantified using AI algorithms integrated with a 3D model constructed from UAV-captured images, improving reliability and efficiency. The software application enables users to analyze segments of the 3D model to measure distances between any two points, including elevation changes. This innovation eliminates the need for manual muck pile measurements, accelerates the measurement process, and enhances the precision of the activities. Several iterations of the measured muck pile are presented in Figure 13.

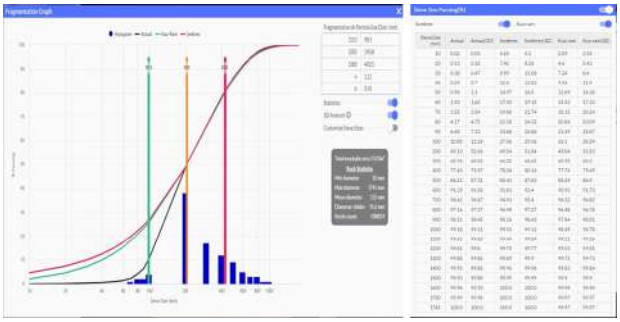

Figure 12. Fragmentation graphs and mean fragmentation sizes based on SWEBREC, KUZ-RAM and actual

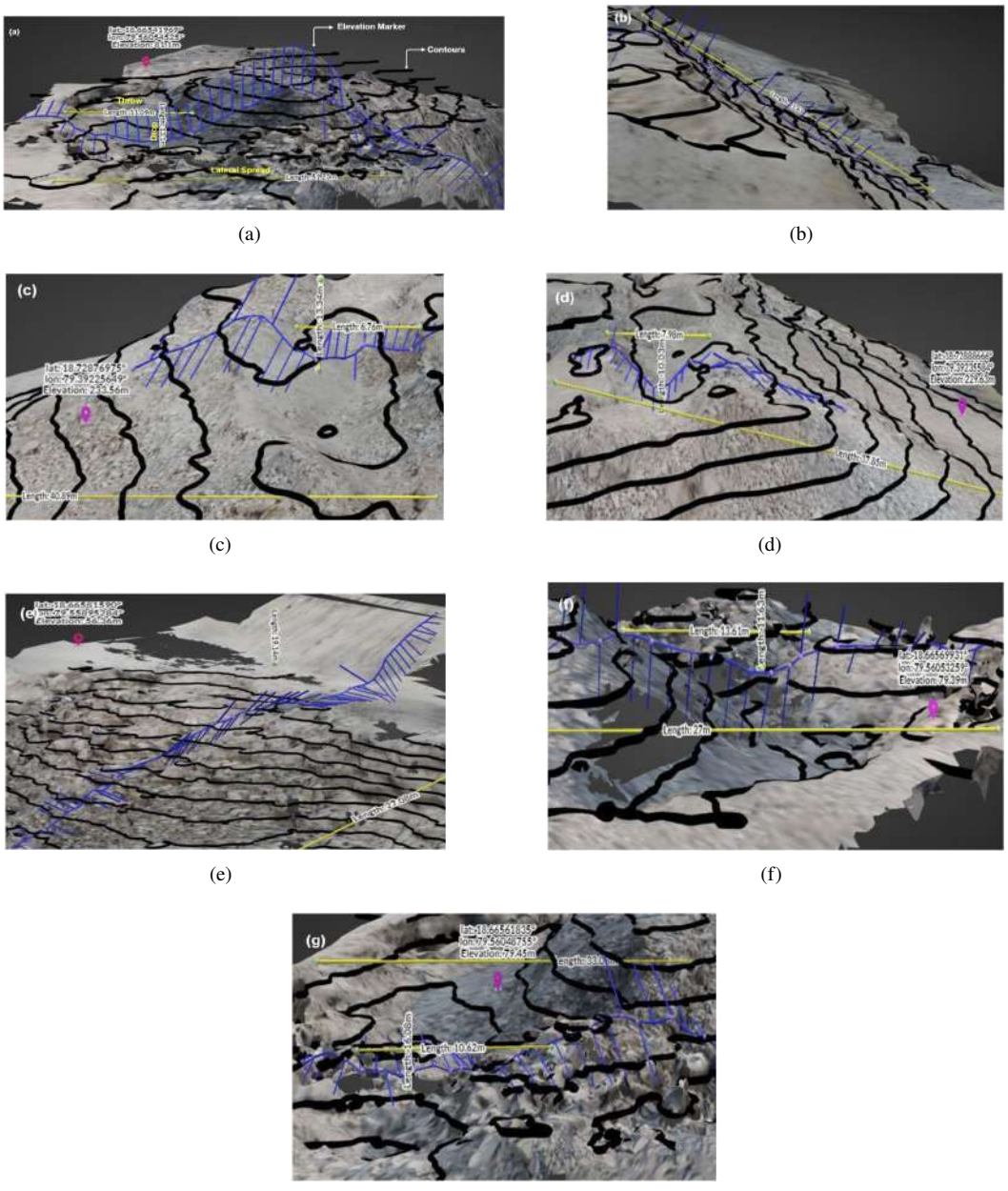

Figure 13. Muck pile characteristics, throw, drop, and lateral spread measurement in software using aerial photographs captured by UAV presented for a few random blasts

AI employs the U-Net convolutional neural network model to generate a flattened 3D model of the bench with joints and visualize fragmentation elevations of the muck pile. The convolutional layer serves as the initial step in the network, utilizing a filter or neuron that interacts with a subset of the input data pixels, depending on the dimensions of the filter (kernel). This kernel or filter is advantageous for various tasks such as image sharpening, blurring, and edge detection. As the kernel moves over the images, it multiplies the values in the filter by the corresponding pixel values in the image. The resulting products are summed to produce a single number, which contributes to the next convolution layer. Subsequently, a maximum pooling layer is applied to reduce the spatial size of the representation, thereby decreasing the number of parameters and computations within the network.

4 Results and Discussion

4.1 Impact of Firing Pattern on Muck Pile Characteristics

The results in Figure 14 indicate that the V firing pattern achieves a drop of 3 meters, a throw of 5.9 meters, and a lateral spread of 19.3 meters, making it particularly effective for optimizing rock fragmentation and displacement. This pattern's perpendicular alignment to the free face allows for precise, controlled detonation timing, leading to ideal in-flight collisions among rock fragments. This dynamic breaks the rock into well-sized fragments, enhancing lateral spread while keeping vertical displacement to a minimum. The V pattern also reduces burden and increases spacing, resulting in less confinement around blast holes, enabling more effective lateral energy dissipation and controlled fragmentation. This minimizes excessive drop depths, producing a stable working surface that aids excavator efficiency, as the shallow 3-meter drop allows for easier access, reducing repositioning needs and streamlining loading cycles.

In contrast, the diagonal firing pattern produced a deeper drop of 11 meters, a throw of 5.3 meters, and a lateral spread of 15 meters, while the line pattern resulted in a maximum drop of 12 meters, a throw of 4.1 meters, and a lateral spread of 13 meters. These configurations, with their oblique and linear firing sequences, direct more energy vertically, leading to deeper drop zones and limited lateral spread, which can hinder excavation and equipment mobility. Overall, the V firing pattern proves to be the most effective choice when excavation efficiency and bench stability are key priorities.

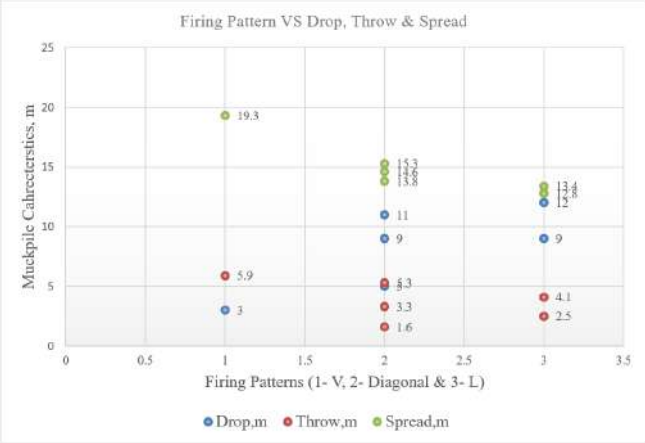

Figure 14. Relationship between the firing pattern and muck pile characteristics

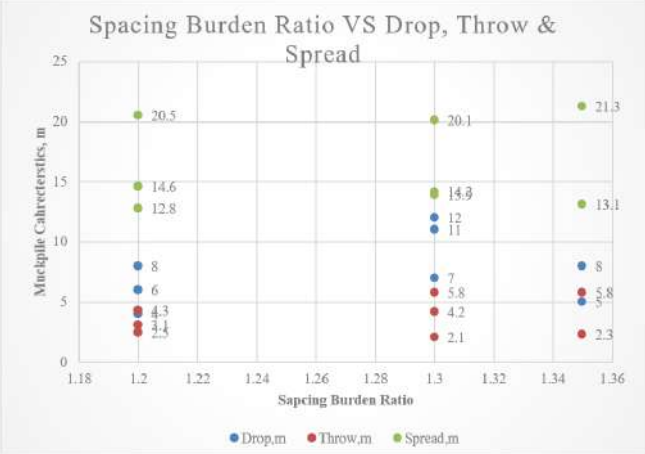

Figure 15. Relationship between the S/B ratio and muck pile characteristics

4.2 Impact of S/B Ratio on Muck Pile Characteristics

The observed results with varying S/B ratios in Figure 15 can be explained through energy distribution and rock fragmentation principles. A lower S/B ratio (1.2) concentrates explosive energy vertically, leading to a higher drop but reduced lateral spread and throw, limiting excavation efficiency. Increasing the ratio to 1.3 distributes energy more evenly, enhancing throw and lateral spread but causing an excessive vertical drop, which can lead to inefficiencies in excavation. In contrast, a ratio of 1.35 optimizes energy use by balancing vertical drop (around 5 meters) with enhanced lateral spread (21 meters), ensuring more effective rock fragmentation and displacement. This ratio reduces excessive drop and improves muck pile stability and excavator performance, while maximizing lateral spread for better operational efficiency and reduced energy waste. The 1.35 S/B ratio thus provides a more effective and economical solution for blast design by maximizing horizontal displacement and optimizing vertical fragmentation, leading to improved overall productivity.

4.3 Impact of Decking Length on Muck Pile Characteristics

Decking length influence, as shown in Figure 16, which refers to the distance between explosive charges in a blast hole, plays a crucial role in how energy is distributed throughout the rock mass. When the decking length is shorter, such as 1 meter, the explosive energy is concentrated over a smaller vertical zone, resulting in a more controlled release of energy and leading to an optimal vertical drop (10 meters), horizontal throw (5 meters), and lateral spread (15 meters). Shorter decking lengths allow for better coupling between adjacent charge sections, enhancing vertical fragmentation and creating a stable muck pile for easier excavation. As the decking length increases to 1.5 meters and 2 meters, the energy is spread over a larger vertical distance, which increases the drop (12 meters at 1.5 meters and 5 meters at 2 meters), throw (6 meters at 1.5 meters and 14 meters at 2 meters), and lateral spread (16 meters at 1.5 meters and 22 meters at 2 meters).

However, the larger decking length reduces the coupling between charges, causing excessive horizontal energy distribution and increasing lateral spread at the cost of reduced vertical fragmentation. The 1-meter decking length achieves a finer balance of both vertical and horizontal energy distribution, ensuring efficient fragmentation and a stable muck pile, while longer decking lengths, despite enhanced lateral spread and throw, reduce overall blast efficiency for excavation due to less effective vertical fragmentation.

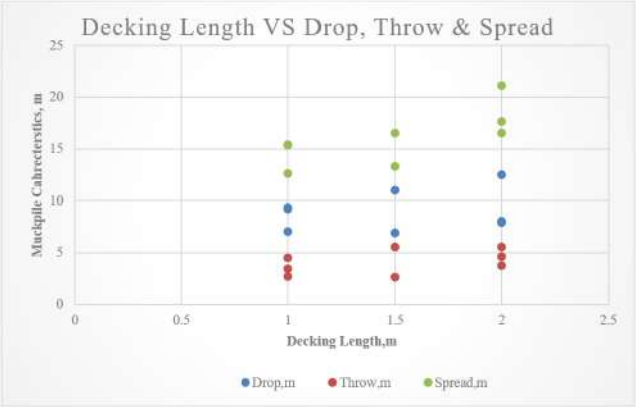

Figure 16. Relationship between the decking length and muck pile characteristics

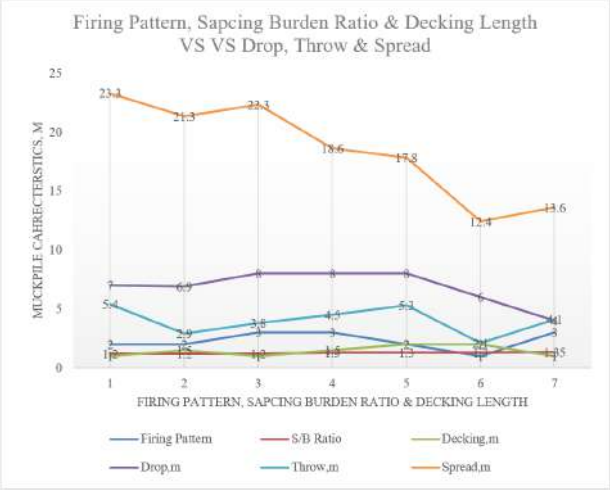

Figure 17. Relationship between combined blast design parameters and muck pile characteristics

4.4 Impact of Cumulative Impact of V Firing Pattern, S/B Ratio and Decking Length on Muck Pile Characteristics

The observed optimal muck pile characteristics in Figure 17, including reduced drop, controlled throw, and enhanced lateral spread, can be explained through the principles of explosive energy distribution and rock fragmentation dynamics. A decking length of 1 meter allows for a more concentrated release of explosive energy over a shorter vertical distance, ensuring better coupling between charge sections. This concentration of energy in a controlled vertical zone leads to a more efficient rock fragmentation, resulting in a smaller drop of less than 4 meters. The reduced drop minimizes the creation of oversized fragments and reduces the risk of unstable muck piles, enhancing excavation efficiency.

A S/B ratio of 1.35 further optimizes energy distribution by ensuring that explosive energy is effectively shared between the vertical and horizontal directions, leading to a balanced lateral spread of more than 15 meters. This ratio prevents excessive vertical energy dissipation, ensuring effective horizontal displacement while maintaining control over fragmentation. The V-shaped firing pattern optimizes the directional energy release, which enhances lateral spread while minimizing excessive throw. This pattern ensures that the energy is directed efficiently, creating a muck pile that is both stable and well-distributed, making it ideal for excavation and loading with shovels. Together, these parameters result in a blast that is both safe and economical, providing optimal fragmentation and reducing the need for secondary blasting while improving operational efficiency.

5 Conclusion

In this study, UAVs play a crucial role in capturing high-quality muck pile photographs, which are essential for characterizing key blast results such as drop, throw, and lateral spread. PCA, performed using XLSTAT, is instrumental in identifying and selecting the most influential blast design parameters affecting the blast outcomes. AI tools were effectively used to design blasts based on insights derived from the baseline study and PCA results. A special AI tool within Strayos software was also utilized, which is unique in its ability to characterize key blast parameters, including throw, drop, and lateral spread.

The results from this study unequivocally demonstrate that the V firing pattern is the optimal choice for controlled rock fragmentation and efficient excavation. This results in well-sized fragments with a 3-meter drop, a 5.9-meter throw, and a 19.3-meter lateral spread, improving muck pile stability and operational efficiency. The S/B ratio of 1.35 optimizes energy distribution, balancing vertical drop (5 meters) with enhanced lateral spread (21 meters). This ratio reduces vertical energy dissipation, improving fragmentation and operational efficiency. A decking length of 1 meter further enhances performance by concentrating explosive energy in a smaller vertical zone, ensuring controlled fragmentation and a stable muck pile.

These findings underline the importance of combining the V-firing pattern, S/B ratio of 1.35, and 1-meter decking length to achieve the most efficient and economical blast design. Such an approach not only improves excavation efficiency but also contributes to the economic viability of the operation by minimizing the need for secondary blasting and optimizing loading cycles. The reduced vertical drop and enhanced lateral spread allow for efficient rock displacement, improving the overall productivity of the mining operation and reducing the operational costs associated with excavation and loading.

Data Availability

Data will be available on reasonable request from the corresponding authors.

Conflicts of Interest

The authors declare no conflict of interest.

References

[1] B. S. Choudhary, "Effect of blast induced rock fragmentation and muckpile angle on excavator performance in surface mines," *Min. of Min. Depos.*, vol. 13, no. 3, pp. 119–126, 2019. https://www.example.com/choudhary2019

[2] D. Zou and D. Zou, "Explosives," *Theor. Tech. Rock Excav. Civ. Eng.*, pp. 105–170, 2017. https://www.example.com/zou2017

[3] P. Xu, R. Yang, J. Zuo, C. Ding, C. Chen, Y. Guo, and Y. Zhang, "Research progress of the fundamental theory and technology of rock blasting," *Int. J. Miner. Metall. Mater.*, vol. 29, no. 4, pp. 705–716, 2022. https://www.example.com/xu2022

[4] F. Ouchterlony, "Influence of blasting on the size distribution and properties of muckpile fragments: A state-of-the-art review," *Blast. Size Distrib. Muckpile Frag.*, 2003.

[5] Q. Liu, F. Shi, X. Wang, and M. Zhao, "Statistical estimation of blast fragmentation by applying 3D laser scanning to muck pile," *Shock Vib.*, 2022. https://doi.org/10.1155/2022/3757561

[6] I. Brunton, D. Thornton, R. Hodson, and D. Sprott, "Impact of blast fragmentation on hydraulic excavator dig time," in *Fifth Large Open Pit Mining Conference*, Kalgoorlie, WA, 2003, pp. 39–48.

[7] S. Hanspal, M. Scoble, and Y. Lizotte, "Anatomy of a blast muckpile and its influence on loading machine performance," in *21st Annual Conference on Explosives and Blasting Techniques*, Nashville, TN (United States), 1995, pp. 57–67.

[8] P. Rai, "Evaluation of effect of some blast design parameters on fragmentation in open cast mine," Ph.D. dissertation, Banaras Hindu University, Varanasi, 2002.

[9] C. K. McKenzie, "A review of the influence of gas pressure on block stability during rock blasting," in *Explo-99*, 1999, pp. 173–179.

[10] M. S. Stagg, R. Otterness, and D. F. Siskind, "Effects of blasting practices on fragmentation," in *the 33rd U.S. Symposium on Rock Mechanics (USRMS)*, Santa Fe, New Mexico, 1992, pp. 313–322.

[11] W. R. Adamson, C. R. Scherpenisse, and J. C. Diaz, "The use of blast monitoring modeling technology for the optimization of development blasting," in *Explo-99*, 1999, pp. 35–41.

[12] S. S. Kanchibotla, W. Valery, and S. Morrell, "Modelling fines in blast fragmentation and its impact on crushing and grinding," in *Explo-99*, 1999, pp. 137–144.

[13] S. Bhandari, *Engineering Rock Blasting Operations*. Rotterdam, The Netherlands, 1997.

[14] S. N. Chandrahas, B. S. Choudhary, N. S. R. Krishna Prasad, V. Musunuri, and K. K. Rao, "An investigation into the effect of rockmass properties on mean fragmentation," *Arch. Min. Sci.*, vol. 66, pp. 561–578, 2021. https://doi.org/10.1155/2021/8819618

[15] N. S. Chandrahas, B. S. Choudhary, and M. S. Venkataramayya, "Competitive algorithm to balance and predict blasting outcomes using measured field data sets," *Comput. Geosci.*, vol. 27, pp. 1087–1110, 2023. https://doi.org/10.1007/s10596-023-10254-x

[16] M. Naresh, N. S. Sri Chandrahas, G. Praful Kumar, and K. Sravan Kumar, "Harmonizing blasting efficiency: A case study on evaluation and optimization of fragmentation size and ground vibration," *J. Inst. Eng. India Ser. D*, 2024. https://doi.org/10.1007/s40033-024-00730-8

[17] N. S. Chandrahas, B. S. Choudhary, and M. S. Venkataramayya, "Firing pattern and spacing burden ratio selection in jointed overburden benches using unmanned aerial vehicle and artificial intelligence based tool," in *Proceedings of the Second International Conference on Emerging Trends in Engineering (ICETE 2023)*, 2023, p. 134. https://doi.org/10.2991/978-94-6463-252-1_134

[18] D. Ramesh, N. S. Chandrahas, M. S. Venkataramayya *et al.*, "Effects of spacing-to-burden ratio and joint angle on rock fragmentation: An unmanned aerial vehicle and AI approach in overburden benches," *Acadlore Trans. Geosci.*, vol. 2, no. 3, pp. 155–166, 2023. https://doi.org/10.56578/atg020303

[19] T. Pradeep, N. S. Chandrahas, and Y. Fissha, "A principal component-enhanced neural network framework for forecasting blast-induced ground vibrations," *J. Civ. Hydraul. Eng.*, vol. 2, no. 4, pp. 206–219, 2024. https://doi.org/10.56578/jche020402

[20] N. S. Chandrahas, Y. Fissha, B. S. Choudhary, B. O. Taiwo, M. S. Venkataramayya, and T. Adachi, "Experimental data-driven algorithm to predict muckpile characteristics in jointed overburden bench using unmanned aerial vehicle and AI tools," *Int. J. Min. Reclam. Environ.*, vol. 38, no. 8, pp. 642–676, 2024. https://doi.org/10.1080/17480930.2024.2340876

[21] N. S. Chandrahas, B. S. Choudhary, M. S. Venkataramayya *et al.*, "An inventive approach for simultaneous prediction of mean fragmentation size and peak particle velocity using futuristic datasets through improved techniques of genetic XG boost algorithm," *Min. Metall. Explor.*, vol. 41, pp. 2391–2405, 2024. https://doi.org/10.1007/s42461-024-01045-8

[22] S. Chandrahas, B. S. Choudhary, M. S. Venkataramayya, Y. Fissha, and B. O. Taiwo, "An investigation of the cumulative impact of decking length and firing pattern on blasting results," *J. Min. Environ.*, vol. 16, no. 1, pp. 97–110, 2024. https://doi.org/10.22044/jme.2024.14555.2743

[23] N. S. Chandrahas, B. S. Choudhary, M. S. Venkataramayya, Y. Fissha, and N. R. Cheepurupalli, "Ai-driven analysis of rock fragmentation: The influence of explosive charge quantity," *Acadlore Trans. Geosci.*, vol. 3, no. 3, pp. 123–134, 2024. https://doi.org/10.56578/atg030301

[24] R. F. Chiappetta, D. G. Borg, and V. A. Sterner, *Explosives and Rock Blasting*. Dallas: Atlas Powder Company, 1987.

[25] M. Frimpong, K. Kabongo, and C. Davies, "Diggability, a measure of dragline effectiveness and productivity," *Int. Soc. Exp. Engs.*, pp. 95–104, 1996.

[26] A. Abd Elwahab, E. Topal, and H. D. Jang, "Review of machine learning application in mine blasting," *Arab. J. Geosci.*, vol. 16, no. 2, p. 133, 2023. https://doi.org/10.1007/s12517-023-11237-z

[27] K. Rajwar, K. Deep, and S. Das, "An exhaustive review of the metaheuristic algorithms for search and optimization: Taxonomy, applications, and open challenges," *Artif. Intell. Rev.*, vol. 56, pp. 13 187–13 257, 2023. https://doi.org/10.1007/s10462-023-10470-y

[28] K. S. Lee and Z. W. Geem, "A new meta-heuristic algorithm for continuous engineering optimization: Harmony search theory and practice," *Comput. Methods Appl. Mech. Eng.*, vol. 194, no. 36-38, pp. 3902–3933, 2005. https://doi.org/10.1016/j.cma.2004.09.007

[29] S. Desale, A. Rasool, S. Andhale, and P. Rane, "Heuristic and meta-heuristic algorithms and their relevance to the real world: A survey," *Int. J. Comput. Eng. Res. Trends*, vol. 2, no. 5, pp. 296–304, 2015.

[30] S. Zhang, X. Ma, and J. Yan, "Effects of blast design parameters on fragmentation in an open pit mine," *Min. Metall. Explor.*, vol. 35, no. 3, pp. 415–425, 2018.

[31] S. Bhandari, "Burden and spacing relationship in the design of blasting pattern," in *16th Symposium on Rock Mechanics*, Minneapolis, MN, USA, 1975, pp. 333–343.

[32] S. Prasad, B. S. Choudhary, and A. K. Mishra, "Effect of blast design parameters on blast induced rock fragmentation size – A case study," in *International Conference on Deep Excavation, Energy Resources and Production (DEEP16)*, Kharagpur, India, 2017, pp. 24–26.

[33] N. S. Smith, "An investigation of the effects of blast hole confinement on generation of ground vibration in bench blasting," SMI Grant Section, Final report for blasting research, 1976.

[34] Z. X. Zhang, Y. Qiao, L. Y. Chi, and D. F. Hou, "Experimental study of rock fragmentation under different stemming conditions in model blasting," *Int. J. Rock Mech. Min. Sci.*, vol. 143, p. 104797, 2021. https://doi.org/10.1016/j.ijrmms.2021.104797

[35] Q. Wu, Y. Huang, and C. Tang, "Effects of joint spacing on rock fragmentation and muck pile characteristics in open-pit mining," *Minerals*, vol. 9, no. 9, p. 554, 2019. https://doi.org/10.3390/min9090554

[36] Q. Chen, Y. Zhang, and X. Shi, "Influence of joint orientation on muck pile fragmentation under blasting," *Int. J. Min. Sci. Technol.*, vol. 27, no. 5, pp. 833–838, 2017. https://doi.org/10.1016/j.ijmst.2017.09.018

[37] P. A. Cundall, "Numerical modelling of jointed and faulted rock," in *Mechanics of Jointed and Faulted Rock*, H. P. Rossmanith, Ed. CRC Press, 1990.

[38] J. M. Belland, "Structure as a control in rock fragmentation coal lake iron Ore deposited," *Can. Min. Metall. Bull.*, vol. 59, no. 647, pp. 323–328, 1968.

[39] Q. Li, S. Liu, and Y. Wang, "Effects of bedding plane orientation on particle size distribution and shape of muck pile fragmentation," *Adv. Civ. Eng.*, vol. 2021, p. 6651309, 2021.